Accepted manuscript:

Trace element and Nd isotope composition of shallow seawater prior to the Great Oxidation Event: Evidence from stromatolitic bioherms in the Paleoproterozoic Rooinekke and Nelani Formations, South Africa

By

Katharina Schier[a,□], Michael Bau[a], Carsten Münker[b], Nicolas Beukes[c], Sebastian Viehmann[a,1]

a Department of Physics and Earth Sciences, Jacobs University Bremen, Campus Ring 1, 28759 Bremen, Germany
b Institut für Geologie und Mineralogie, Universität zu Köln, Zülpicher Straße 49b, 50674 Cologne, Germany
c DST-NRF Centre of Excellence for Integrated Mineral and Energy Resource Analysis, Department of Geology, University of Johannesburg, Auckland Park, 2092 Johannesburg, South Africa
1 Current address: Department of Geodynamics and Sedimentology, University of Vienna, Althanstraße 14, 1090 Vienna, Austria.

https://doi.org/10.1016/j.precamres.2018.07.014

Received 31 January 2018; Received in revised form 22 June 2018; Accepted 17 July 2018
Available online 18 July 2018 (Embargo: 24 months)

Trace element and Nd isotope composition of shallow seawater prior to the Great Oxidation Event: Evidence from stromatolitic bioherms in the Paleoproterozoic Rooinekke and Nelani Formations, South Africa

Katharina Schier, Michael Bau, Carsten Münker, Nicolas Beukes, Sebastian Viehmann

PII: S0301-9268(18)30069-X
DOI: https://doi.org/10.1016/j.precamres.2018.07.014
Reference: PRECAM 5134

To appear in: *Precambrian Research*

Received Date: 31 January 2018
Revised Date: 22 June 2018
Accepted Date: 17 July 2018

Please cite this article as: K. Schier, M. Bau, C. Münker, N. Beukes, S. Viehmann, Trace element and Nd isotope composition of shallow seawater prior to the Great Oxidation Event: Evidence from stromatolitic bioherms in the Paleoproterozoic Rooinekke and Nelani Formations, South Africa, *Precambrian Research* (2018), doi: https://doi.org/10.1016/j.precamres.2018.07.014

Trace element and Nd isotope composition of shallow seawater prior to the Great Oxidation Event: Evidence from stromatolitic bioherms in the Paleoproterozoic Rooinekke and Nelani Formations, South Africa

Katharina Schier[a]*, Michael Bau[a], Carsten Münker[b], Nicolas Beukes[c] and Sebastian Viehmann[a, 1]

[a]*Department of Physics and Earth Sciences, Jacobs University Bremen, Campus Ring 1, 28759 Bremen, Germany*

[b]*Institut für Geologie und Mineralogie, Universität zu Köln, Zülpicher Straße 49b, 50674 Cologne, Germany*

[c]*DST-NRF Centre of Excellence for Integrated Mineral and Energy Resource Analysis, Department of Geology, University of Johannesburg, Auckland Park, 2092 Johannesburg, South Africa*

** corresponding author, tel.: +49 421 200 3154, E-Mail address: k.schier@jacobs-university.de (Katharina Schier)*

[1]current address: *Department of Geodynamics and Sedimentology, University of Vienna, Althanstraße 14, 1090 Vienna, Austria*

ABSTRACT

Pure, stromatolitic limestones from the ~2.44 to 2.43 Ga old Rooinekke Formation, Transvaal Supergroup (South Africa), provide unique insight into the geochemistry of Paleoproterozoic shallow seawater and, therefore, into the evolution of ambient redox-levels of the Earth's atmosphere-hydrosphere system. In contrast to the stromatolitic Klipput dolostones from the overlying Nelani Iron Formation (IF), the stromatolitic Rooinekke limestones do not show post-depositional alteration and are virtually free of detrital contamination. This makes them excellent geochemical archives of proxies of ambient shallow-marine Transvaal seawater. Shale-normalized (SN) rare earth element and yttrium (REY) patterns of pure Rooinekke limestones show seawater-like REY distributions with positive La_{SN} and Gd_{SN} anomalies, super-chondritic Y/Ho ratios and a depletion of the light (LREY) relative to the heavy REY_{SN} (HREY). However, the lack of negative Ce_{SN} anomalies implies that redox conditions at the Earth's surface were not oxidizing enough to stabilize significant amounts of Ce(IV). In contrast to the majority of Archean marine chemical sediments, the pure Early Paleoproterozoic Rooinekke limestones lack positive Eu_{SN} anomalies, suggesting that the fraction of REY derived from high-temperature (>250°C) hydrothermal fluids in shallow Rooinekke seawater was negligible. The predominance of continental sources in the geochemical REY budget of Rooinekke seawater is corroborated by unradiogenic $\varepsilon Nd_{(2.44\ Ga)}$ values close to those of contemporaneous upper crustal material. The Rooinekke limestones, therefore, reveal the absence of a high-temperature hydrothermal component from *shallow* seawater already at least 100 million years prior to the Great Oxidation Event. In contrast, older chemical sediments from the Transvaal Supergroup, such as the Campbellrand carbonates and the Penge and Kuruman IFs, show positive Eu_{SN} anomalies and more radiogenic $\varepsilon Nd_{(t)}$ values, indicating a significant contribution of mantle-

derived REY via high-temperature hydrothermal fluids to the late Neoarchean shallow marine REY inventory on the Kaapvaal Craton. The declining impact of high-temperature hydrothermal fluids on surface seawater, that is recorded by the late Neoarchean to Paleoproterozoic shallow water Transvaal carbonates, is similar to the general trend of decreasing positive Eu_{SN} anomalies with decreasing depositional age, that is observed in Eoarchean to Proterozoic IFs which recorded the composition of deeper marine waters.

Keywords: Paleoproterozoic, seawater, REY, stromatolites, Great Oxidation Event

1 INTRODUCTION

Stromatolitic carbonates are shallow marine biogenic chemical sediments that if pure and pristine, may be excellent archives of geochemical proxies that recorded the physico-chemical conditions prevailing in the oceans of the Early Earth. Since stromatolites commonly formed within the marine photic zone, their trace element and isotope composition may provide insight into the composition of ambient marine surface water (Kamber and Webb, 2001; Kamber et al., 2004; Kamber et al., 2014; Van Kranendonk et al., 2003; Webb and Kamber, 2000) which in turn reflects the local conditions in the atmosphere-hydrosphere system at the time of carbonate formation. A similar approach has widely been used for banded iron formations (BIFs) as archives of ambient seawater chemistry, but BIFs usually represent deeper water masses (e.g., Alibert and McCulloch, 1993; Alexander et al., 2009; Bau and Alexander, 2009; Planavsky et al., 2010; Viehmann et al., 2015a, b; and references therein; for an exceptional shallow water BIF see e.g. Alexander et al., 2008).

The rare earth elements and yttrium (REY) are commonly used as geochemical proxies to constrain the paleo-redox-level and element sources and fluxes to the Early Earth's ocean (e.g., Alexander et al., 2008; Bau and Dulski, 1996; Bau and Möller, 1993; Bolhar et al., 2004; Derry and Jacobsen, 1990; Viehmann et al., 2015a, b; 2016; Webb and Kamber, 2000). They are also powerful tools to distinguish between pure marine chemical sediments and those that were affected by syn- and/or post-depositional processes such as contamination by detrital aluminosilicates and diagenetic or metamorphic overprint (e.g., Bau, 1993; Bau and Alexander, 2009; Kamber et al., 2014; Viehmann et al., 2015a, b; 2016; Webb and Kamber, 2000). The REY budget of marine chemical sediments such as cherts, BIFs and also stromatolitic carbonates, is very sensitive to detrital contamination due to the very low REY concentrations in the chemically precipitated endmember (e.g., Bau, 1993; Webb and Kamber, 2000). Therefore, only pure chemical sediments can be used to reconstruct paleoenvironmental conditions and thorough screening of a sample set and subsequent focusing on the purest and most pristine samples is of utmost importance. However, it is well established that the REY distribution of such pure and pristine Archean and Paleoproterozoic marine sedimentary carbonates and BIFs represents that of the water mass from which the respective chemical sediment precipitated (e.g., Alexander et al., 2008; Bau and Dulski, 1996; Bolhar et al., 2004; Derry and Jacobsen, 1990; Kamber and Webb, 2001; Kamber et al., 2004; Nothdurft et al., 2004; Planavsky et al., 2010; Van Kranendonk et al., 2003; Viehmann et al., 2013; 2016). Due to coherent REY partitioning between sedimentary carbonates and ambient seawater, fractionation of the REY during their incorporation into the crystal lattice of stromatolitic carbonates is minor, which makes them an excellent archive of the REY distribution in ambient seawater (e.g., Kamber et al., 2004; Webb and Kamber, 2000; Tostevin et al., 2016). In contrast to Phanerozoic marine sedimentary

carbonates, there often exist only minor differences between the shale normalized (subscript SN; shale is PAAS - Post Archean Australian Shale - of McLennan, 1989) REY patterns of Early Precambrian limestones and dolostones (e.g., Bau and Alexander, 2006; Bau et al., 1999; Kamber and Webb, 2001; Tsikos et al., 2001), suggesting that these dolostones were either primary precipitates from seawater or that dolomitization occurred at a very early stage of diagenesis from pore waters that showed seawater-like REY distribution.

In natural environments, the REY are typically trivalent. Under oxic conditions, however, Ce may be oxidized on particle surfaces, within alkaline waters or during interaction with biogenic ligands such as siderophores, and following oxidation, Ce is often fixed in less-soluble Ce(IV) compounds and preferentially removed from or kept in solution; in any case, the stabilization of Ce(IV) compounds results in decoupling of Ce from its trivalent REY neighbours (Elderfield, 1988; Krämer et al., 2017; Möller and Bau, 1993; Piepgras and Jacobsen, 1992; Zhang and Nozaki, 1996; 1998). In most situations, this produces a negative Ce_{SN} anomaly in weathering solutions, such as soil solutions and river waters, and ultimately in modern oxic seawater (e.g., Bau and Koschinsky, 2009). In contrast, Eu^{3+} is (partially) reduced under hot (> 250°C) and acidic conditions (e.g., Bau, 1991; and references therein) and, therefore, may be decoupled from the other REY in high-temperature hydrothermal fluids, resulting in a positive Eu_{SN} anomaly due to preferential partitioning of the trivalent REY relative to divalent Eu into secondary alteration minerals and due to enhanced Cl^- complexation of Eu^{2+} (Allen and Seyfried, 2005; Bau and Dulski, 1999; Douville et al., 1999; Haas et al., 1995; Schmidt et al., 2010). The impact of such high-temperature hydrothermal fluids on seawater chemistry can be tracked by the presence of positive Eu_{SN} anomalies in marine chemical sediments such as BIFs (e.g., Danielson et al., 1992; Derry and Jacobsen, 1990; Viehmann et al., 2015b) or stromatolitic

carbonates (e.g., Kamber and Webb, 2001; Van Kranendonk et al., 2003). Using this proxy, it had been suggested that the REY contribution of high-temperature hydrothermal fluids to the elemental budget of the Precambrian oceans was significantly higher than it is today (e.g., Alexander et al., 2009; Bau and Möller, 1993; Danielson et al., 1992; Fryer, 1977; Viehmann et al., 2015b) and may even have been controlled by geodynamic processes of the Earth's interior and linked with peak episodes of severe magmatic activity such as mantle plumes (Isley and Abbott, 1999; Viehmann et al., 2015b). The anoxic conditions in (deep) Archean seawater prevented the scavenging of REY onto metal (oxyhydr)oxide particles at and close to the hydrothermal vent sites (which restricts hydrothermal REY input into the modern, well-oxygenated oceans).

Beyond the application of the REY as a tool to constrain the environmental conditions in seawater, the Nd isotope composition of pure marine chemical sediments (which are characterized by very low abundances of elements commonly associated with detrital aluminosilicates, such as Al, Zr and Hf; e.g., Bau, 1993) can be used to constrain the sources of the marine REY inventory (e.g., Alexander et al., 2008; 2009; Alibert and McCulloch, 1993; Viehmann et al. 2013; 2015a, b; 2016). This is possible because Nd is particle-reactive and, hence, has a marine residence time shorter than the ocean mixing time. The Nd isotope composition of seawater, therefore, is not homogenous, but represents a local rather than a global signal. The modern oceans receive REY input exclusively from continental sources, which is reflected by a non-radiogenic Nd isotope composition, i.e. negative εNd values (Frank, 2002; Goldstein and O'Nions, 1981; Lacan and Jeandel, 2005; Piepgras and Wasserburg, 1980). In contrast, Early Precambrian chemical sediments recorded a more radiogenic Nd isotope signature (i.e. positive $\varepsilon Nd_{(t)}$ values), which is composed of a mixture of terrigenous and mantle-like Nd

delivered to ancient seawater via high-temperature hydrothermal fluids that altered young oceanic crust (and, possibly, the overlying sediment pile). The hydrothermal REY flux was much larger in the Archean than it is today, producing a more radiogenic Nd isotope ratio (e.g., Alexander et al., 2009; Bau et al., 1997; Derry and Jacobsen, 1990; Frei and Polat, 2007; Kamber and Webb, 2001; Miller and O'Nions, 1985; Viehmann et al., 2013; 2015b; 2016).

We here report REY and Nd isotope data for 2.44 to 2.43 Ga old stromatolitic limestones and dolostones from the Early Paleoproterozoic Rooinekke and Nelani Iron Formations, respectively. They are part of the Koegas Subgroup of the Transvaal Supergroup (South Africa), which was deposited shortly before the Great Oxidation Event (GOE; Holland, 2002). The aim is to characterize the physico-chemical conditions in shallow marine waters and to constrain the REY sources to the Early Paleoproterozoic ocean shortly before the Earth surface system experienced the profound oxygenation event during which evidence of mass-independent fractionation of sulfur isotopes disappeared from the geological record. For this purpose, the present sample set was screened for the purest and most pristine samples based on a combination of major and trace element abundances, oxygen isotope compositions and REY distributions. Only the most pristine samples were then used as archives of Early Paleoproterozoic seawater chemistry.

2 GEOLOGICAL SETTING AND SAMPLES

The Rooinekke and Nelani Iron Formations constitute the uppermost known part of the Koegas Subgroup of the Ghaap Group of the Transvaal Supergroup, in the Griqualand West Area (Northern Cape Province, South Africa; Figs. 1 and 2). The succession has undergone only minor deformation and burial metamorphism that did not exceed greenschist facies conditions

(Beukes, 1978; 1983). The Koegas Subgroup is overlain with sharp low angle erosional unconformity by the glaciogenic Makganyene Diamictite (Beukes, 1983; Beukes and Smit, 1987), which forms the base of the Postmasburg Group of the Transvaal Supergroup in Griqualand West (Fig. 2a). The diamictite is considered an analogue to other ~2.4 to 2.2 Ga old Huronian glacial deposits (Polteau et al., 2006), representing a global glaciation event extending to low latitudes, i.e. a potential "Snowball Earth" which can be traced in the worldwide sedimentary record (Evans et al., 1997; Hoffmann and Schrag, 2002; Kirschvink et al., 2000). Hence, the sedimentary rocks of the Koegas Subgroup, including the Rooinekke and Nelani Iron Formations, were deposited shortly before the ~2.33 Ga GOE which was tracked on the Archean-Proterozoic Kaapvaal Craton by the disappearance of the MIF-S (mass-independent fractionation of sulfur isotopes) signal across the Duitschland/Rooihoogte Formations (Guo et al., 2009; Luo et al., 2016).

The depositional age of the Rooinekke-Nelani iron formation succession is poorly defined. The best estimate is based on the age of the youngest zircon extracted from an interbedded thin stilpnomelane tuff bed by Gutzmer and Beukes (1998). The U-Pb age of this zircon that is 98 % concordant, was determined by SHRIMP to be 2415 ± 6 Ma. However, the data shows signs of lead loss and if correction is made for that, the age shifts to approximately 2436 Ma (Gutzmer and Beukes, 1998). Another zircon in the same sample with 98 % concordance gave an age of 2434 ± 8 Ma (Gutzmer and Beukes, 1998). If these zircons are considered related to the volcanic event that gave rise to the ash-fall tuff then they may approximate the depositional age of the iron formation succession. However, there are a significant number of zircons present in the tuff bed with older ages and especially a large population of zircons with ages around 2500 Ma. Clearly, thus, some zircons in the tuff bed were

inherited from older sources so that the 2436 Ma age at best represents a maximum age of deposition of the Rooinekke-Nelani iron formation succession.

A recent age of 2426 ± 3 Ma published by Gumsley et al. (2017) on baddeleyite extracted from a sill intruded in the overlying Ongeluk Lava above the Makganyene Diamictite would place deposition of the iron formation succession in the interval between 2436 and 2426 Ma. Thus, indications are that deposition took place prior to the GOE as defined by the final disappearance of MIF-S in the Duitschland-Rooihoogte succession of the Pretoria Group of the Transvaal Supergroup at ~2330 Ma (Guo et al., 2009; Luo et al., 2016). It also predates deposition of the Kalahari Manganese Field that may represent a pre-GOE transient event of oxygenation in Earth's history (Bau and Alexander, 2006; Gumsley et al., 2017). The depositional age of the Hotazel Iron Formation is estimated to be 2413 ± 15 Ma by Gutzmer and Beukes (1998), and the conformably overlying Mooidraai Dolomite was dated to 2394 ± 26 Ma by Bau et al. (1999) and at 2392 ± 23 by Fairey et al. (2013).

In the Rooinekke and Nelani Iron Formation succession, stromatolitic bioherms with patchy discontinuous lateral extent are developed at three stratigraphic levels, namely at the base of the Rooinekke Iron Formation, at the top of the basal Klipput shale member of the Nelani Iron Formation, and at the top of the latter iron formation (Fig. 2b). The latter unit is the highest known to be preserved below the erosional unconformity at the base of the Makganyene Diamictite. In this study, sedimentary carbonates were sampled from two of the stromatolitic bioherm horizons, namely that at the base of the Rooinekke Iron Formation on the farm Taaiboschfontein (S28°50'17.8" E23°07'59.0") and that at the top of the Klipput member of the Nelani Iron Formation on the farm Sandridge (S28°49'25" E22°39'22"; Figs. 1 and 2 and Figs. S1 and S2 of the supplementary material). The bioherms have a domal shape and are either

composed of homogenous massive carbonate or show a distinct lamination at the millimeter scale. They vary in thickness from a few centimeters up to several meters. Large thicknesses are, however, due to inheritance of domal shapes of which the actual synoptic relief is typically less than 50 cm. The bioherms interfinger laterally with iron-rich shale and chert and are draped by carbonate facies BIF in both cases (Figs. S1 and S2 of the supplementary material). For purpose of reference, the samples taken at Taaiboschfontein will be referred to as Rooinekke bioherms or limestones and those at Sandridge as Klipput bioherms or dolostones.

3 ANALYTICAL TECHNIQUES

Homogenous hand specimens without any weathering crusts and/or secondary veins were crushed and milled using an agate ball mill. For samples that showed distinct lamination, single layers were sampled parallel to the laminae using a microdrill with a diamond-bearing drill head (diameter of microdrillcore was 1.5 mm). These microdrillcores were broken down to smaller chips using an agate mortar. Crushed and milled samples were dissolved at high pressure and temperature in an acid mix of suprapure conc. HCl, HNO_3 and HF (3:1:1) in a Picotrace digestion system for three days at 180°C following the procedure described in detail by Alexander (2008). After complete dissolution, the acid-sample-mixture was evaporated to incipient dryness at 200°C, the samples were dissolved and evaporated twice in 5ml suprapure conc. HCl and then redissolved in 0.5M HNO_3 + 0.5% HCl for major and trace element determination.

All major and trace element data are given in Tables S6, S7, S8 and S9 of the supplementary material. Major and trace element concentrations were determined by inductively coupled plasma optical emission spectrometry (ICP-OES) and mass spectrometry (ICP-MS),

respectively, at Jacobs University Bremen. One limestone (JLs-1) and one dolomite (JDo-1) standard reference material were included in the sample set from the Koegas Subgroup in order to monitor analytical quality (Table S6 of the supplementary material).

Trace element data for the REY are shown normalized to Post-Archean Australian Shale (PAAS; data from McLennan, 1989) and anomalies are calculated after Bau and Dulski (1996) and Bolhar et al. (2004) as follows: $(La/La^*)_{SN} = La_{SN}/(3Pr_{SN}-2Nd_{SN})$; $(Ce/Ce^*)_{SN} = Ce_{SN}/(2Pr_{SN}-Nd_{SN})$; $(Eu/Eu^*)_{SN} = Eu_{SN}/(0.67Sm_{SN}+0.33Tb_{SN})$; $(Gd/Gd^*)_{SN} = Gd_{SN}/(2Tb_{SN}-Dy_{SN})$.

The Sm-Nd isotope compositions of *pure* stromatolitic Rooinekke limestones were determined by isotope dilution and Thermo Finnigan Neptune MC-ICPMS analyses at the Steinmann Institut Bonn in the joint clean laboratory facilities of the University of Bonn and the University of Cologne. Aliquots of 150 to 500 mg of homogenous sample powder and freshly drilled and homogenized sample material (stromatolitic laminae) adjacent to the microdrilled trace element aliquot from the same individual stromatolitic layer (samples SA-ST-18c_F, SA-ST1-10a_F, SA-ST1-10c_F, SA-ST1-5b_F, SA-ST1-20a_F, SA-ST1-20b_F) were dissolved with 6ml of 6M HCl for circa 5 to 10 minutes until the first reaction stopped. The solutions were heated for 12h at 120°C, subsequently cooled down and spiked with ^{180}Ta-^{180}Hf-^{176}Lu-^{94}Zr and ^{149}Sm-^{150}Nd isotope tracers. 1ml of concentrated HF and $HClO_4$ was added to the solutions for another 12 hours to ensure complete digestion. The solutions were evaporated, treated with 2ml HNO_3 + trace HF and subsequently evaporated again. The final step involved sample-spike equilibration with 6 M HCl + 0.06 M HF for another 12 hours and ion exchange separation. Before the latter step, a 10% aliquot was taken from the solution for trace element determination on the samples (sample names SA-ST1-XX_F, Table S6 of the supplementary material).

Analytical quality was assessed by comparison of Sm and Nd concentrations being measured at Jacobs University Bremen and at the University of Bonn (Table S8 of the supplementary material). Samarium and Nd concentrations typically show deviations of <5% for Sm and <10% for Nd. All analytical procedures follow protocols that are described in detail elsewhere (Münker et al., 2001; Pin and Zalduegui, 1997; Weyer et al., 2002). $^{143}Nd/^{144}Nd$ ratios were mass bias corrected to a $^{146}Nd/^{142}Nd$ of 0.7219 using the exponential law. The LaJolla and JNd1 Nd standards were measured with a $^{143}Nd/^{144}Nd$ of 0.511731 (n=1) and 0.511963 ±13 (n=4), respectively and all data are given to a $^{143}Nd/^{144}Nd$ value of 0.511859 of the LaJolla. The Nd blank of this procedure was measured with 134 pg and the typical external reproducibility for $^{147}Sm/^{144}Nd$ is ±0.2% (2σ). For initial εNd calculations of this sample set and recalculation of literature data, the ^{147}Sm decay constant of $6.54 \cdot 10^{-12}$ (Lugmair and Marti, 1978) and the CHUR parameters from Bouvier et al. (2008) were applied.

Oxygen and carbon isotope compositions were determined at the University of Göttingen using a Thermo Kiel IV carbonate preparation device in combination with a Finnigan DeltaPlus mass spectrometer following the methods of McCrea (1950). The calculation of $\delta^{18}O_{calcite}$ and $\delta^{18}O_{dolomite}$ was done using the acid fractionation factors of Kim et al. (2007) and Rosenbaum and Sheppard (1986), respectively. All data are reported relative to Pee Dee Belemnite (PDB).

4 RESULTS

4.1 Major elements and strontium

Based on their major element chemical composition, stromatolitic carbonate samples from the Rooinekke Iron Formation can be classified as limestones, whereas those from the Klipput Member of the Nelani Formation are dolostones (Fig. 3; data in Table S6 of the

supplementary material). We did not observe dolostone at the former or limestones at the latter location.

Calcium concentrations are between 6.2 and 38.7 wt % and 18.6 to 19.8 wt. % in the Rooinekke limestones and the Klipput dolostones, respectively (Table S6 of the supplementary material). Accordingly, Mg concentrations are low in the limestones (0.4 to 4.2 wt %) and higher in the dolostones (18.7 to 19.2 wt. % Mg; Table S6 of the supplementary material). The limestones are characterized by Fe contents between 1.0 and 20.1 wt. %; the dolostones show Fe contents of 2.0 to 3.8 wt. % (Table S6 of the supplementary material). Manganese concentrations in the limestones range between 0.37 and 1.9 wt. % and between 0.37 and 0.42 wt % in the dolostones. Some of the limestones are silicified with calculated SiO_2 contents up to 56.5 wt % (Table S6 of the supplementary material). The degree of silicification was determined assuming that all Ca, Mg, Mn and Fe is present as carbonate, Al as Al_2O_3 and P as P_2O_5. The difference between the sum of these compounds and the total equates to the SiO_2 content of the respective sample. For the dolostones Ca and Mg were assumed to be present as dolomite.

The Sr concentrations of the Rooinekke limestones range from 126 - 353 ppm (Table S6 of the supplementary material) and they are, therefore, depleted in Sr relative to modern marine calcites, which may contain up to ~1000 ppm Sr (e.g., Veizer, 1983). The Klipput dolostones, however, are even more depleted in Sr than the limestones and show concentrations between 46 and 60 ppm Sr (Table S6 of the supplementary material).

4.2 Rare earth elements and other trace elements

The Rooinekke stromatolitic limestones show REY_{SN} patterns that are sub-parallel to those of modern seawater with positive La_{SN} ($(La/La^*)_{SN}$: 0.99-1.75), Gd_{SN} ($(Gd/Gd^*)_{SN}$: 1.17-1.76) and Y_{SN} anomalies (i.e. super-chondritic Y/Ho ratios between 48.8 and 93.8), and Yb_{SN}/Pr_{SN} ratios above unity (Yb_{SN}/Pr_{SN}: 2.12 - 8.93), indicating light REY_{SN} ($LREY_{SN}$) depletion relative to the heavy REY_{SN} ($HREY_{SN}$) (Fig. 4a). Neither Ce_{SN} nor large Eu_{SN} anomalies ($(Eu/Eu^*)_{SN}$: 1.12 - 1.40, mean: 1.27; n= 21, Fig. S3 of the supplementary material) can be observed in the Rooinekke limestones (Fig. 4a). The Eu_{SN} anomalies are slightly higher than Eu_{CN} anomalies (0.68 - 0.89); subscript CN: normalized to chondrite of Anders and Grevesse (1989), because normalizing to PAAS introduces a "normalization artifact", as PAAS itself has a negative Eu_{CN} anomaly.

Limestone sample SA-ST1-1_K (open symbols in Fig. 4a) is an exception with respect to its REY_{SN} distribution and trace element concentrations, as it has a rather flat REY_{SN} pattern and shows the highest REY concentrations as well as anomalously high concentrations of Al (3550 ppm), Zr (23.8 ppm) and Hf (0.58 ppm) relative to the other samples (Table S6 of the supplementary material). Aluminum and Zr concentrations for the rest of the limestone samples range from 332 ppm to 2250 ppm and from 0.389 ppm to 10.2 ppm, respectively (Fig. 5a; data in Table S6 of the supplementary material).

In marked contrast to the Rooinekke limestones, the REY_{SN} patterns of the Klipput dolostones are considerably different and dissimilar to those of modern seawater (Fig. 4b). They lack any La_{SN} ($(La/La^*)_{SN}$: 0.90 - 0.99), Gd_{SN} ($(Gd/Gd^*)_{SN}$: 1.10 - 1.36) or large positive Y_{SN} anomalies (Y/Ho: 33.1 - 38.9; Fig. 4b and Figs. S3, S4 and S5 of the supplementary material) and do not show any systematic strong $LREY_{SN}$ depletion relative to the $HREY_{SN}$ (Yb_{SN}/Pr_{SN}: 0.74-1.96). However, they do show slight positive Eu anomalies ($(Eu/Eu^*)_{SN}$: 1.19-1.47, mean:

1.44; n=4, Fig. S3 of the supplementary material). Aluminum and Zr concentrations range between 665 ppm and 2970 ppm and 0.422 ppm and 3.06 ppm, respectively (Figs. 5a and b, Figs. S4 and S5 of the supplementary material, data in Table S6 of the supplementary material).

4.3 Neodymium isotopes

Neodymium isotope compositions were determined for pure and pristine Rooinekke limestone samples (see section 5.1: Sample purity) that show seawater-like REY_{SN} patterns. Ratios of $^{147}Sm/^{144}Nd$ range between 0.11669 and 0.13842 and show consistently negative $\varepsilon Nd_{(2.44\ Ga)}$ values between -3.01 ± 0.2 and -0.94 ± 0.1, except for one outlier (SA-ST1-10c_F) with an $\varepsilon Nd_{(2.44\ Ga)}$ value of +0.46 ± 0.2 (Figs. 6a and b; data in Table S7 of the supplementary material).

4.4 Carbon and Oxygen Isotopes

Carbon and oxygen isotope compositions determined for a subset of the samples (Fig. 7a and b; data in Table S9 of the supplementary material) confirm the distinction between the Rooinekke limestones and the Klipput dolostones and closely agree with the results for Rooinekke calcites and Klipput dolomites sampled by Frauenstein et al. (2009) on the farms Taaiboschfontein and Sandridge, respectively.

The Klipput dolostones show the heaviest values for carbon and oxygen with $\delta^{13}C_{PDB}$ ranging from -1.53 to -0.23 ‰ and $\delta^{18}O_{PDB}$ values between -9.97 and -7.72 ‰ (Fig. 7a). The Rooinekke limestones are isotopically lighter and show a larger spread in $\delta^{13}C$ values ($\delta^{13}C_{PDB}$: -8.14 to -2.86 ‰; $\delta^{18}O_{PDB}$: -14.2 to -12.5 ‰; Fig. 7a and b) than the Klipput dolostones.

5 DISCUSSION

5.1 Sample purity

Elements commonly associated with detrital aluminosilicates, such as Al and Zr, show low concentrations in the Rooinekke limestones and Klipput dolostones. After screening the sample set for these elements and considering the REY_{SN} distribution of the samples, we conservatively applied "cut-off values" of 2000 ppm Al and 5 ppm Zr to exclude samples possibly affected by detrital aluminosilicates (Fig. 5a). Samples with Al and/or Zr concentrations above these threshold values (SA-ST1-1_K, SA-ST1-20b_K, SA-ST1-18b_K, SA-ST2-1a and SA-ST2-1b) are shown as open symbols and were excluded from the subsequent data evaluation, because they are not pure enough to be used as a reliable archive of the geochemical proxies examined in this study. To confirm the effectiveness of the measures taken, two mixing lines were calculated between two pure Rooinekke limestone endmembers (Fig. 5b) and an endmember of contemporaneous upper continental crust with assumed Al and Nd concentrations of 90,000 ppm and 25 ppm (Transvaal shale endmember; Fig. 5b), respectively. Three of the samples previously excluded based on their Al and Zr contents (SA-ST1-1_K, SA-ST2-1a and SA-ST2-1b) are indeed slightly shifted towards the Transvaal shale endmember along these mixing lines (Fig. 5b). The composition of the rest of the samples does not follow the calculated mixing lines, corroborating their purity and, therefore, their suitability as archives of geochemical proxies for ambient seawater chemistry.

5.2 Depositional environment and diagenesis

The distribution of the major elements and carbon and oxygen isotope compositions reveal differences in the degree of diagenetic overprint between the Rooinekke limestones and

the Klipput dolostones. The strongly elevated Mg content and the depletion of Sr in the dolostones relative to the limestones suggests post-depositional alteration of these carbonates during dolomitization, which commonly involves the depletion of Sr due to its large ionic radius and its lower partition coefficient for dolomite than for calcite (Brand and Veizer, 1980). Oxygen isotope compositions of the dolostones are, therefore, assumed to be of secondary origin, and do not allow us to draw reliable conclusions with regard to the isotope composition of ambient seawater, because oxygen isotopes tend to shift towards lighter values during diagenetic processes due to the elevated temperature of the interacting fluids (Hoefs, 1997). Generally, oxygen isotopes are much more mobile and, therefore, more sensitive to diagenetic alteration than carbon isotopes due to buffering of the latter by carbonate carbon (Jacobsen and Kaufman, 1999). The very light oxygen isotope composition of the Rooinekke limestones, which is positively correlated with the calculated SiO_2 content of the samples (data in Tables S6 and S9 of the supplementary material), and Klipput dolostones, therefore, indicate post-depositional resetting of the oxygen isotope system. Such resetting may result, for example, from the interaction of the limestones and dolostones with low-$\delta^{18}O$ glacial meltwaters at elevated temperatures, as observed by Zakharov et al. (2017) for hydrothermally altered rocks associated with intrusions of Paleoproterozoic age on the Baltic Shield.

In contrast to the Klipput dolostones, the Rooinekke limestones do not show evidence of strong post-depositional dolomitization. Although some samples show slight enrichment in Mg, which may represent the onset of secondary dolomitization, this process did not reach the extent shown by the Klipput dolostones, which is corroborated by the higher Sr concentrations of the Rooinekke limestones as compared to the dolostones (Table S6 of the supplementary material).

This suggests that the carbon isotope compositions of the Rooinekke limestones may also be less affected than those of the Klipput dolostones.

Rooinekke limestones show lighter carbon isotope compositions than Klipput dolostones (Figs. 7a and b), which is in agreement with those of other carbonates of similar age (Shields and Veizer, 2002) and similar origin (Fairey et al., 2013; Frauenstein et al., 2009). This lighter carbon isotope composition could be explained by diagenetic redox-reactions involving the oxidation of organic carbon compounds by co-deposited Fe_2O_3 and the formation of C-isotopically light Fe- and Ca-Fe-carbonates during diagenesis (e.g. Fairey et al., 2013; Smith et al., 2013). The negative trend between Fe/Ca ratios and $\delta^{13}C_{PDB}$ in the Rooinekke limestones supports this hypothesis (Fig. 7b).

In spite of the wide range of carbon isotope compositions and Fe/Ca ratios (Fig. 7a and b), all Rooinekke limestones show very similar REY_{SN} patterns, suggesting that the process(es) that controlled carbon isotope composition and Fe/Ca ratios did not affect the REY distribution. The lack of correlation between calculated SiO_2 content and Y/Ho ratios, La_{SN} anomalies, Eu_{SN} anomalies and $(Yb/Pr)_{SN}$ ratios (Table S6 of the supplementary material) indicates that silicification also did not modify the REY distribution.

The REY are usually very robust during dolomitization processes (e.g., Banner et al., 1988; Parekh et al., 1977; Webb et al., 2009), as they reside within the carbonate crystal lattice (Zhong and Mucci, 1995), such that a considerable fraction of the rock would have to undergo complete dissolution in order to change its REY distribution (e.g., Banner et al., 1988; Webb and Kamber, 2000). Moreover, whereas REY_{SN} patterns of Phanerozoic dolostones usually deviate strongly from those of contemporaneous limestones and seawater, *Early Precambrian* limestones

and dolostones have been found to often show very similar REY distributions (e.g., Bau and Alexander, 2006).

The Paleoproterozoic Klipput dolostones are rather exceptional from other dolostones in the Transvaal Supergroup, as their REY_{SN} patterns differ from those of the slightly older Rooinekke limestones (Figs. 4a and b). This either suggests (i) that they formed in a restricted basin or lagoon with riverine influx and limited exchange with the open ocean, (ii) that they represent freshwater precipitates or (iii) that they formed from a limestone precursor during secondary dolomitization in the presence of pore waters. Considering the similar range of Al, Th, Zr, Hf, Rb and Cs concentrations in the purest limestones and dolostones formation in a lagoon or a landlocked freshwater environment, i.e. in close proximity to a landmass, appears to be unlikely. Moreover, the inorganic particle load of river waters, which shows a shale-like REY_{SN} pattern is subject to aggregation, removal and deposition already in the low-salinity part of estuaries (Merschel et al., 2017a; Tepe and Bau, 2016). This produces low-salinity estuarine waters, which already show a REY_{SN} signature similar to that of seawater. Therefore, even *if* the detritus-free Klipput dolostones formed in a depositional environment with a substantial contribution from river waters, they should show a seawater-like REY_{SN} distribution rather than the shale-like REY_{SN} signature of river particles. This, however, is not observed in our samples and we, therefore, rather consider the REY distribution of the Klipput dolostones a feature that developed during dolomitization. However, whatever may have caused the REY_{SN} patterns of the Klipput carbonates, these dolostones should not be used as archives of the REY composition of shallow marine Paleoproterozoic seawater, which is the focus of this study. In contrast, the Rooinekke limestones, after a thorough screening procedure which takes into account geological context, major and trace element composition, can serve as excellent geochemical archives of

ambient seawater chemistry and allow us to geochemically characterize shallow Rooinekke seawater.

5.3 The evolution of the REY inventory of Transvaal seawater

In contrast to modern seawater, Rooinekke surface seawater, as revealed by the pure Rooinekke limestones, lacked a negative Ce_{SN} anomaly (Fig. 4a). This indicates that the environmental conditions in the shallow surface water at ~2.44 to 2.43 Ga, i.e. before the GOE, were still too reducing to oxidize Ce^{3+} and fix a significant fraction of Ce in insoluble Ce(IV) compounds. Hence, there was no decoupling of Ce from its REY neighbours during terrestrial weathering, riverine transport, and estuarine and marine processes in the continental hinterland and the coastal areas, respectively, of the Kaapvaal Craton. This does not support the notion of "whiffs" of oxygen or the pervasive oxygenation of the ocean margins prior to the GOE, that had been suggested based on the Mo-Re systematics of the somewhat older (~2.5 Ga) Mount McRae shale, Hamersley Basin, Australia (Anbar et al., 2007), and of the 2.6 - 2.5 Ga old black shales from the Campbellrand-Malmani Subgroup, South Africa (Kendall et al. 2010). However, in the absence of a comparative study of the sensitivity of the paleo-redox proxies any further interpretations is premature.

The lack of positive Eu_{SN} anomalies (Figs. 4a and 6b and Fig. S3 of the supplementary material) which are indicative of high-temperature hydrothermal contributions to the REY inventory of seawater, suggests that such high-temperature hydrothermal fluids did not significantly influence the REY budget of shallow Rooinekke seawater. This is further corroborated by the negative, i.e. unradiogenic $\varepsilon Nd_{(2.44\ Ga)}$ values (Figs. 6a and b) of the Rooinekke limestones, which are close to published data for shales from the Transvaal

Supergroup (recalculated from data of Dia et al., 1990 and Jahn and Condie, 1995). The $\varepsilon Nd_{(2.44\ Ga)}$ values of the limestones overlap with the least negative $\varepsilon Nd_{(2.44\ Ga)}$ values of Transvaal shales (range: -2.6 ± 0.2 to -5.7 ± 0.6), which represent the upper crustal component of the Kaapvaal Craton at the time of Rooinekke stromatolitic limestone formation. This suggests that mantle-derived Nd was not a major component in the total Nd budget of shallow Rooinekke seawater.

The Nd isotope composition of the Transvaal shales represents that of the average eroded hinterland material (i.e. that of detrital aluminosilicates), whereas the Nd isotope composition of the pure Rooinekke limestones should be close to that of the dissolved and truly dissolved (i.e., that pass a 0.2 µm and 1 KDa filter, respectively) REY fractions in river waters, as the latter control REY input into ambient seawater. However, the Transvaal shales (detrital component) are on average about 2.7 epsilon units less radiogenic than the Rooinekke limestones (dissolved component). Such an offset is also observed in modern river systems and is attributed to incongruent weathering of silicate minerals (Merschel et al., 2017b; Viers and Wasserburg, 2004) or to an over-representation of (ultra)mafic material with more positive εNd values in the suspended particle load relative to the weathered and eroded bulk continental crust (Garçon et al., 2014).

Comparing the REY_{SN} patterns and the Nd isotope composition of Rooinekke stromatolitic limestones to those of older chemical sedimentary rocks from the Transvaal Supergroup reveals a significant difference. Although the REY_{SN} patterns of Rooinekke limestones closely resemble those of older Transvaal limestones, dolostones and BIFs (Figs. 4a, c and d), they lack the positive Eu_{SN} anomalies that are ubiquitous in the older formations (Rooinekke $(Eu/Eu^*)_{SN}$: 1.15 - 1.40; Figs. 4c and d, Fig. 6b, older Transvaal $(Eu/Eu^*)_{SN}$: 1.10 -

2.26; Figs. 4c and d, Fig. 6b). These positive Eu_{SN} anomalies in the older Campbellrand Subgroup (2.52 Ga) reveal a significant REY contribution from high-temperature hydrothermal fluids. We emphasize that, although this contribution appears to have become more pronounced with increasing depositional depth (Kamber and Webb, 2001), even the stromatolitic shallow water Campbellrand carbonates yield a positive Eu_{SN} anomaly. The $\varepsilon Nd_{(2.521\ Ga)}$ values of the Campbellrand carbonates show a much wider range and a more radiogenic maximum (-4.5 to +2.0; Figs. 6a and b) than those of the Rooinekke limestones (-3.01 ± 0.2 and -0.94 ± 0.1; Figs. 6a and b), possibly due to variable contributions from high-temperature hydrothermal sources to the former (Kamber and Webb, 2001). The Penge (2.480 Ga old; Nelson et al., 1999) and Kuruman (2.460 Ga old; Pickard, 2003) iron formations (IF) which also pre-date the Rooinekke Formation, also show positive Eu_{SN} anomalies and more radiogenic $\varepsilon Nd_{(t)}$ values (Bau and Dulski, 1996; Bau et al., 1997; Figs. 6a and b).

After the deposition of the Rooinekke limestones the positive Eu_{SN} anomalies did not reappear, as shown by shallow water limestones and dolostones from the Mooidraai Formation (represented by the grey bar in Fig. 6b; Bau et al., 1999; Bau and Alexander, 2006; Tsikos et al., 2001), which are about 40 million years younger than the Rooinekke carbonates.

The declining influence of high-temperature hydrothermal fluids, that is recorded by the Transvaal marine chemical sedimentary succession, may be explained assuming that the Transvaal ocean had been chemically stratified with only limited exchange between these water masses. The deeper waters were influenced by high-temperature hydrothermalism and carried the corresponding chemical characteristics (a radiogenic εNd signature and positive Eu_{SN} anomalies), whereas shallower waters lack these features. Such a stratification was proposed by several geochemical studies on the Transvaal sedimentary sequence (e.g. Sumner, 1997; Kamber and

Webb, 2001; von Blanckenburg et al., 2008; Kurzweil et al., 2016). If such stratification had persisted at 2.44 Ga this would be in line with the lack of Eu_{SN} anomalies in Rooinekke shallow water limestones. However, some of the older Campbellrand limestones and dolostones are also stromatolitic and formed in the photic zone, i.e. in shallow waters, suggesting that water column stratification cannot be the sole reason for the lack of Eu_{SN} anomalies in the Rooinekke carbonates. In addition, the Rooinekke basin needed to have been a semi-enclosed basin with only very limited exchange with open ocean deep waters which carried the high-temperature hydrothermal geochemical signal. Another, and perhaps more likely, explanation is a general decline of marine high-temperature hydrothermal activity through time. This is in accord with results from modelling, which propose a decrease of astenospheric mantle temperatures due to more stable thermal conditions in the Earth's mantle, which occurred at the transition from the Archean to the Proterozoic (Davies, 2008; Campbell and Griffith, 2014). The resulting decline of previously intense volcanic activity, that was responsible for the eruption of hot, high-Mg mafic volcanics, has been traced in the sedimentary record which shows that (i) average Archean upper continental crust was more mafic than it is today (Condie, 1993) and (ii) Ni delivery to the oceans from weathering of ultramafic rocks decreased significantly after ~2.7 Ga (as recorded by lower Ni/Fe ratios in BIFs; Konhauser et al., 2009). A decrease in astenospheric mantle temperatures and, therefore, volcanic activity would have resulted in a decline of high-temperature hydrothermal activity at oceanic spreading centres. This in turn, would have triggered a change in the contemporaneous seawater REY geochemistry from an ocean that was strongly impacted by a high-temperature hydrothermal signal to one that gradually lost the respective geochemical characteristics. Such a scenario is similar to that proposed by Viehmann

et al. (2015b) to explain the general trend of decreasing Eu_{SN} anomalies in IFs from the Eoarchean to the Proterozoic.

5 CONCLUSION

Pure (i.e. detritus free) stromatolitic limestones from the ~2.44 to 2.43 Ga old Rooinekke Formation, Transvaal Supergroup (South Africa), show REY_{SN} patterns sub-parallel to those of modern seawater except for the lack of negative Ce_{SN} anomalies. Super-chondritic Y/Ho ratios, positive La_{SN} and Gd_{SN} anomalies, and depletion of $LREY_{SN}$ relative to the $HREY_{SN}$ along with low concentrations of elements typically associated with detrital aluminosilicates (e.g., Al, Zr, Hf) imply that they are pure marine chemical sediments which can be used as archives of proxies for the chemical composition of ambient shallow Rooinekke seawater. The lack of Ce_{SN} anomalies suggests environmental conditions that were not oxidizing enough to decouple Ce from the other REY via the oxidation of Ce^{3+} to $Ce^{4+}$and the subsequent preferential removal of Ce(IV) relative to its REY(III) neighbours. Unradiogenic $\varepsilon Nd_{(2.44\ Ga)}$ values and the lack of positive Eu_{SN} anomalies are consistent with a REY budget of shallow Rooinekke seawater that was mainly derived from low-temperature continental REY sources with no or negligible contributions from a high-temperature hydrothermal mantle source. In contrast, sedimentary carbonates from the older Campbellrand Subgroup reveal such a high-temperature hydrothermal component of mantle-derived REY in shallow seawater, as even stromatolitic (i.e. shallow water) Campbellrand carbonates show positive Eu_{SN} anomalies and more radiogenic $\varepsilon Nd_{(t)}$ values. The Kuruman and Penge iron formations confirm these findings also for late Neoarchean deeper waters, while the younger Mooidraai carbonates, do not show positive Eu_{SN} anomalies and,

therefore, support the notion of a negligible influence of high-temperature hydrothermal fluids on the marine REY budget.

The Rooinekke stromatolitic limestones along with other Transvaal marine chemical sediments, therefore, appear to record a decline of high-temperature hydrothermal mantle contributions to the REY inventory of shallow seawater across the Archean-Proterozoic boundary. This significant change in the Earth system likely resulted from decreasing astenospheric mantle temperatures and depicts a shift towards a seawater REY chemistry dominated by riverine input from continental REY sources already at least 100 million years before the GOE.

ACKNOWLEDGEMENTS

We greatly appreciate the help of Dennis Krämer (Jacobs University Bremen) during sampling and Andreas Pack (Georg-August-Universität Göttingen) and Brian Alexander (Jacobs University Bremen, now Inorganic Ventures Inc., USA) for the analysis of carbon and oxygen isotope compositions of the Rooinekke carbonates and trace elements of the Campbellrand carbonates, respectively. We also thank Katja Schmidt and Gila Merschel for numerous fruitful discussions and their help with the interpretation of Nd isotope data. The comments of Balz Kamber and another anonymous reviewer helped to substantially improve the manuscript; Randall Parrish is thanked for the entire process of editorial handling. This research did not receive any specific grant from funding agencies in the public, commercial, or not-for-profit sectors but benefited from collaboration within the DFG-funded priority program SPP 1833 “Building a Habitable Earth”.

REFERENCES

Allen, D. E. and Seyfried, W. E. (2005): REE controls in ultramafic hosted MOR hydrothermal systems: an experimental study at elevated temperature and pressure. Geochimica et Cosmochimica Acta 69, 675-683.

Alexander, B. (2008): Trace element analysis in geochemical materials using low resolution inductively coupled plasma mass spectrometry (ICPMS), Technical report No. 18. https://opus.jacobs-university.de/frontdoor/index/index/docId/678

Alexander, B., Bau, M., Andersson, P. and Dulski, P. (2008): Continentally-derived solutes in shallow Archean seawater: Rare earth element and Nd isotope evidence in iron formation from the 2.9 Ga Pongola Supergroup, South Africa. Geochimica et Cosmochimica Acta 72, 378-394.

Alexander, B., Bau, M. and Andersson, P. (2009): Neodymium isotopes in Archean seawater and implications for the marine Nd cycle in Earth's early oceans. Earth and Planetary Science Letters 283, 144-155.

Alibert, C. and McCulloch, M. T. (1993): Rare earth element and neodymium isotopic composition of the banded iron-formation and associated shales from Hamersley, Western Australia. Geochimica et Cosmochimica Acta 57, 187-204.

Alibo, D. S. and Nozaki, Y. (1999): Rare earth elements in seawater: Particle association, shale-normalization, and Ce-oxidation. Geochimica et Cosmochimica Acta 63, no. 3/4, 363-372.

Anders, E. and Grevesse, N. (1989): Abundance of the elements: Meteoric and solar. Geochimica et Cosmochimica Acta 53, 197-214.

Banner, J. L., Hanson, G. N. and Myers, W. J. (1988): Rare earth element and Nd isotopic variations in regionally extensive dolomites from the Burlington-Keokuk Formation (Mississippian): Implications for REE mobility during carbonate diagenesis. Journal of Sedimentary Petrology 58, 415-432.

Bau, M. (1991): Rare earth element mobility during hydrothermal and metamorphic fluid-rock interaction and the significance of the oxidation state of europium. Chemical Geology 93, 219-230.

Bau, M. (1993): Effects of syn- and post-depositional processes on the rare-earth element distribution in Precambrian iron-formations. European Journal of Mineralogy 5, 257-267.

Bau, M. and Dulski, P. (1996): Distribution of yttrium and rare-earth elements in the Penge and Kuruman iron-formations, Transvaal Supergroup, South Africa. Precambrian Research 79, 37-55.

Bau, M. and Möller, P. (1993): Rare earth systematics of the chemically precipitated component in Early Precambrian iron formations and the evolution of the terrestrial atmosphere-hydrosphere-lithosphere system. Geochimica et Cosmochimica Acta 57, 2239-2249.

Bau, M. and Dulski, P. (1999): Comparing yttrium and rare earths in hydrothermal fluids from the Mid-Atlantic Ridge: Implications for Y and REE behaviour during near vent mixing and for the Y/Ho ratio of Proterozoic seawater. Chemical Geology 155, 77-90.

Bau, M. and Alexander, B. (2006): Preservation of primary REE patterns without Ce anomaly during dolomitization of Mid-Paleoproterozoic limestone and the potential re-establishment of marine anoxia immediately after the "Great Oxidation Event", South African Journal of Geology 109 (1-2), 81-86.

Bau, M. and Alexander, B. (2009): Distribution of high field strength elements (Y, Zr, REE, Hf, Ta, Th, U) in adjacent magnetite and chert bands and in reference standards FeR-3 and FeR-4 from the Temagami iron-formation, Canada, and the redox level of the Neoarchean ocean. Precambrian Research 174, 337-346.

Bau, M. and Koschinsky, A. (2009): Oxidative scavenging of cerium on hydrous Fe oxide: Evidence from the distribution of rare earth elements and yttrium between Fe oxides and Mn oxides in hydrogenetic ferromanganese crusts. Geochemical Journal 43, 37-47.

Bau, M., Höhndorf, A., Dulski, P. and Beukes, N. J. (1997): Sources of Rare-Earth elements and iron in the Paleoproterozoic iron-formations from the Transvaal Supergroup, South Africa: Evidence from Neodymium isotopes. The Journal of Geology 105, 121-129.

Bau, M., Romer, R. L., Lüders, V. and Beukes, N. J. (1999): Pb, O, and C isotopes in silicified Mooidraai dolomite (Transvaal Supergroup, South Africa): implications for the composition of Paleoproterozoic seawater and 'dating' the increase of oxygen in the Precambrian atmosphere. Earth and Planetary Science Letters 174, 43-57.

Beukes, N. J., (1978): Die karbonaategsteentes en ysterformasies van die Ghaap-Groep van die Transvaal-Supergroep in Noord-Kaapland, Ph.D. Thesis (unpubl.), Rand Afrikaans University, Johannesburg, pp. 580.

Beukes, N. J. (1983): Paleoenvironmental setting of iron-formations in the depositional basin of the Transvaal Supergroup, South Africa. pp. 131-209 in Trendall, A.F., and Morris, R.C., Eds., 'Iron-Formations: Facts and Problems'. Elsevier, Amsterdam.

Beukes, N. J. and Smit, C. A. (1987). New evidence for thrusting in Griqualand West, South Africa: Implications for stratigraphy and the age of red beds. South African Journal of Geology, 90, 378-394.

Bolhar, R., Kamber, B. S., Moorbath, S., Fedo, C. M. and Whitehouse, M. J. (2004): Characterization of early Archean chemical sediments by trace element signatures. Earth and Planetary Science Letters 222, 43-60.

Bouvier, A., Vervoort, J. D. and Patchett, P. J. (2008): The Lu-Hf and Sm-Nd isotopic composition of CHUR: constraints from unequilibrated chondrites and implications for the bulk composition of the terrestrial planets. Earth and Planetary Science Letters 273, 48-57.

Brand, U. and Veizer, J. (1980): Chemical diagenesis of a multicomponent carbonate system. 1. Trace elements. Journal of Sedimentary Petrology 50, 1219-1236.

Campbell, I. H. and Griffith, R. W. (2014): Did the formation of D'' cause the Archean-Proterozoic transition?, Earth and Planetary Science Letters 388, 1-8.

Danielson, A., Möller, P. and Dulski, P. (1992): The europium anomalies in banded iron formations and the thermal history of the oceanic crust. Chemical Geology 97, 89-100.

Davies, G. F. (2008): Episodic layering of the early mantle by the 'basalt barrier' mechanism. Earth and Planetary Science Letters 275, 382-392.

Derry, L. A. and Jacobsen, S. B., (1990): The chemical evolution of Precambrian seawater: evidence from REEs in banded iron formations. Geochimica et Cosmochimica Acta 54, 2965-2977.

Dia, A., Allégre, C. J. and Erlank, A. J. (1990): The development of continental crust through geological time: The South African case. Earth and Planetary Science Letters 98, 74-89.

Douville, E., Bienvenu, P., Charlou, J. L., Donval, J. P., Fouquet, Y., Appriou, P. and Gamo, T. (1999): Yttrium and rare earth elements in fluids from varius deep-sea hydrothermal systems. Geochimica et Cosmochimica Acta 63, 627-643.

Evans, D. A. D., Beukes, N. J. and Kirschvink, J. J. (1997): Low-latitude glaciation in the Paleoproterozoic era. Nature 386, 262-266.

Elderfield, H., Whitfield, J.D. Burton, M. P., Bacon, M. P. and Liss, P. S. (1988): The oceanic chemistry of the rare-earth elements. Philos. Trans. R. Soc. London Ser. A Math. Phys. Sci. 325, 105-126.

Fairey, B., Tsikos, H., Corfu, F. and Polteau, S. (2013): U-Pb systematics in carbonates of the Postmasburg Group, Transvaal Supergroup, South Africa: Primary versus metasomatic controls. Precambrian Research 231, 194-205.

Frank, M. (2002): Radiogenic isotopes: tracers of past ocean circulation and erosional input. Reviews of Geophysics 40, 1-38.

Frauenstein, F., Veizer, J. Beukes, N. J., Van Niekerk, H. S. and Coetzee, L. L. (2009): Transvaal Supergroup carbonates: Implications for Paleoproterozoic $\delta^{18}O$ and $\delta^{13}C$ records. Precambrian Research 175, 149-160.

Frei, R. and Polat, A. (2007): Source heterogeneity for the major components of ~3.7 Ga Banded Iron Formations (Isua Greenstone Belt, Western Greenland): Tracing the nature of interacting water masses in BIF formation. Earth and Planetary Science Letters 253, 266-281.

Fryer, B. J. (1977): Rare earth evidence in iron-formations for changing Precambrian oxidation states. Geochimica et Cosmochimica Acta 41, 361-367.

Garçon, M., Chauvel, C., France-Lanord, C., Limonta, M. and Garzanti, E. (2014): Which minerals control the Nd-Hf-Sr-Pb isotopic compositions of river sediments?, Chemical Geology 364, 42-55.

Goldstein, S. L. and O'Nions, R. K. (1981): Nd and Sr isotopic relationships in pelagic clays and ferromanganese deposits. Nature 292, 324-327.

Gumsley, A. P., Chamberlain, K. R., Bleeker, W., Söderlund, U., de Kock, M. O., Larsson, E. R., and Bekker, A. (2017): Timing and tempo of the Great Oxidation Event. Earth and Planetary Science Letters 114, no. 8, 1811-1816.

Guo, Q., Strauss, H., Kaufman, A. J., Schröder, S., Gutzmer, J. Wing, B., Baker, M. A., Bekker, A., Jin, Q., Kim, S.-T., and Farquhar, J. (2009): Reconstructing Earth's surface oxidation across the Archean-Proterozoic transition. Geology 37, 399-402; doi: 10.1130/G25423A.1

Gutzmer, J. and Beukes, N. J. (1998): High grade manganese ores in the Kalahari manganese field: characterisation and dating of ore forming events, Unpublished Report. Rand Afrikaans University, Johannesburg.

Haas, J. R., Shock, E. L. and Sassani, D. C. (1995): Rare-earth elements in hydrothermal systems – estimates of standard partial molal thermodynamic properties of aqueous complexes of the rare-earth elements at high pressures and temperatures. Geochimica et Cosmochimica Acta 59 (21), 4329-4350.

Hoefs, J. (1997): Stable Isotope Geochemistry. Springer, Berlin/Heidelberg, 201 pp.

Hoffman, P. F. and Schrag, D. P. (2002): The Snowball Earth hypothesis: testing the limits of global change. Terra Nova 14, 129-155.

Holland, H. D. (2002): Volcanic gases, black smokers, and the Great Oxidation Event. Geochimica et Cosmochimica Acta 66, 3811-3826.

Isley, A. E. and Abbott, D. H. (1999): Plume-related mafic volcanism and the deposition of banded iron formation. Journal of Geophysical Research 104, 15461-15477.

Jacobsen, S. B. and Kaufman, A. J. (1999): The Sr, Ca and O isotopic evolution of Neoproterozoic seawater. Chemical Geology 161, 37-57.

Jahn, B.-M. and Condie, K. C. (1995): Evolution of the Kaapvaal Craton as viewed from geochemical and Sm-Nd analyses of intracratonic pelites. Geochimica et Cosmochimica Acta 59, no. 11, 2239-2258.

Kamber, B. S. and Webb, G. E. (2001): The geochemistry of late Archaean microbial carbonate: Implications for ocean chemistry and continental erosion history. Geochimica et Cosmochimica Acta 65, 2509-2525.

Kamber, B. S., Bolhar, R. and Webb, G. E. (2004): Geochemistry of late Archaean stromatolites from Zimbabwe: evidence for microbial life in restricted epicontinental seas. Precambrian Research 132, 379-399.

Kamber, B. S., Webb, G.E. and Gallagher, M. (2014): The rare earth element signal in Archaean microbial carbonate: information on ocean redox and biogenicity. Journal of the Geological Society, London 171, 745-763.

Kendall, B., Reinhard, C. T., Lyons, T., Kaufman, A. J., Poulton, S. W. and Anbar, A. D. (2010): Pervasise oxygenation along late Archean ocean margins. Nature Geoscience 3 (9), 647-652.

Kim, S., Mucci, A. and Taylor, B. E. (2007): Phosphoric acid fractionation factors for calcite and aragonite between 25 and 75 °C: revisited. Chemical Geology 246, 135-146.

Kirschvink, J. L., Gaidos, E. J., Bertani, L. E., Beukes, N. J., Gutzmer, J., Maepa, L. N. and Steinberger, R. E. (2000): Paleoproterozoic Snowball Earth: extreme climatic and geochemical change and its biological consequences. PNAS 97, 1400-1405.

Konhauser, K. O., Pecoits, E. Lalonde, S. V., Papineau, D., Nisbet, E. G., Barley, M. E., Arndt, N. T., Zahnle, K. and Kamber, B. S. (2009): Oceanic nickel depletion and a methanogen famine before the Great Oxidation Event. Nature 458, 750-754.

Krämer, D., Tepe, N., Pourret, O. and Bau, M. (2017): Negative cerium anomalies in manganese (hydr)oxide precipitates due to cerium oxidation in the presence of dissolved siderophores. Geochimica et Cosmochimica Acta 196, 197-208.

Kurzweil, F., Wille, M., Gantert, N., Beukes, N. J. and Schoenberg, R. (2016): Manganese oxide shuttling in pre-GOE oceans – evidence from molybdenum and iron isotopes. Earth and Planetary Science Letters 452, 69-78.

Lacan, F. and Jeandel, C. (2005): Neodymium isotopes as a new tool for quatifying exchange fluxes at the continent-ocean interface. Earth and Planetary Science Letters 232, 245-257.

Lugmair, G. W. and Marti, K. (1978): Lunar initial 143Nd/144Nd: differential evolution of the lunar crust and mantle. Earth and Planetary Science Letters 39, 349-357.

Luo, G., Ono, S., Beukes, N. J., Wang, D. T., Xie, S. and Summons, R. E. (2016): Rapid oxygenation of Earth's atmosphere 2.33 billion years ago. Science Advances 2, e1600134.

McCrea, J. M. (1950): On the isotopic chemistry of carbonates and a paleotemperature scale. Journal of Chemical Physics 18, 849-857.

McLennan, S.M., (1989): Rare earth elements in sedimentary rocks: Influence of provenance and sedimentary processes, *in* Lipin, B.R. and McKay, G.A., (Eds.): Geochemistry and mineralogy of rare earth elements: Mineralogical Society of America Reviews in Mineralogy Volume 21, p. 169-200.

Merschel, G., Bau, M. and Dantas, E. L. (2017a): Contrasting impact of organic and inorganic nanoparticles and colloids on the behaviour of particle-reactive elements in tropical estuaries: An experimental study. Geochimica et Cosmochimica Acta 197, 1-13.

Merschel, G., Bau, M., Schmidt, K. Münker, C. and Dantas, E. L. (2017b): Hf and Nd isotopes and REY distribution in the truly dissolved, colloidal and particulate loads of rivers in the Amazon Basin, Brazil. Geochimica et Cosmochimica Acta 213, 383-399.

Miller, R. G. and O'Nions, R. K. (1985): Source of Precambrian chemical and clastic sediments. Nature 314, 325-330.

Möller, P. and Bau, M. (1993): Rare-earth patterns with positive Ce anomaly in alkaline waters from Lake Van, Turkey. Earth and Planetary Science Letters 117, 671-676.

Münker, C., Weyer, S., Scherer, E. and Mezger, K. (2001): Separation of high field strength elements (Nb, Ta, Zr, Hf) and Lu from rock samples for MC-ICPMS measurements: Geochemistry Geophysics Geosystems 2, doi: 10.1029/2001GC000183.

Nelson, D. R., Trendall, A. F. and Altermann, W. (1999): Chronological correlations between the Pilbara and the Kaapvaal cratons. Precambrian Research 97, 165-189.

Nothdurft, L. D., Webb, G. E. and Kamber, B. S. (2004): Rare earth element geochemistry of Late Devonian reefal carbonates, Canning Basin, Western Australia: Confirmation of a seawater REE proxy in ancient limestones. Geochmica et Cosmochimica Acta 68, 263-283.

Parekh, P. P., Möller, P., Dulski, P. and Bausch, W. M. (1977): Distribution of trace elements between carbonate and non-carbonate phases of limestone. Earth and Planetary Science Letters 34, 39-50.

Pickard, A. L. (2003): SHRIMP U-Pb zircon ages for the Paleoproterozoic Kuruman Iron Formation, Northern Cape Province, South Africa: Evidence for simultaneous BIF deposition on Kaapvaal and Pilbara cratons. Precambrian Research 125, 275- 315.

Piepgras, A. L. and Jacobsen, S. B. (1992): The behaviour of rare earth elements in seawater: precise determination of variations in the North Pacific water column. Geochimica et Cosmochimica Acta 56, 1851-1862.

Piepgras, D. J. and Wasserburg, G. J. (1980): Neodymium isotopic variations in seawater. Earth and Planetary Science Letters 50, 128-138.

Pin, C. and Zalduegui, J. S. (1997): Sequential separation of light rare-earth elements, thorium and uranium by miniaturized extraction chromatography: application to isotopic analyses of silicate rocks. Analytica Chimica Acta 339, 79-89.

Planavsky, N., Bekker, A., Rouxel, O. J., Kamber, B. S., Hofmann, A., Knudsen, A. and Lyons, T. W. (2010): Rare Earth Element and yttrium compositions of Archean and Paleoproterozoic Fe formations revisited: New perspectives on the significance and mechanisms of deposition. Geochimica et Cosmochimica Acta 74, 6387-6405.

Polteau, S., Moore, J. M. and Tsikos, H. (2006): The geology and geochemistry of the Paleoproterozoic Makganyene diamictite. Precambrian Research 148, 257-274.

Rosenbaum, J. and Sheppard, S. M. F. (1986): An isotopic study of siderites, dolomites and ankerites at high temperatures. Geochimica et Cosmochimica Acta 50, no.6, 1147-1150.

Rudnick, R. L. and Gao, S. (2003): Composition of the continental crust, *in*: Rudnick. R., (Ed.): The crust: Treatise on Geochemistry 3: Amsterdam, Elsevier Science, p.1-64, doi: 10.1016/B0-08-043751-6/03016-4.

Schmidt, K., Garbe-Schönberg, D., Bau, M. and Koschinsky, A. (2010): Rare earth element distribution in >400°C hot hydrothermal fluids from 5°S, MAR: The role of anhydrite in controlling highly variable distribution patterns. Geochimica et Cosmochimica Acta 74, 4058-4077.

Shields, G. and Veizer, J. (2002): The Precambrian marine carbonate isotope database: version 1. Geochemistry, Geophysics, Geosystems 3 (6).

Smith, A. J. B., Beukes, N. J. and Gutzmer, J. (2013): The composition and depositional environments of Mesoarchean iron formations of the West Rand Group of the Witwatersrand Supergroup, South Africa. Economic Geology 108, 111-134.

Sumner, D. Y. and Bowring, S. A. (1996): U-Pb geochronologic constraints on the deposition of the Campbellrand Subgroup, Transvaal Supergroup, South Africa. Precambrian Research 79, 25-35.

Tepe, N. and Bau, M. (2016): Behaviour of rare earth elements and yttrium during simulation of arctic estuarine mixing between glacial-fed river waters and seawater and the impact of inorganic (nano-)particles. Chemical Geology 438, 134-145.

Tostevin, R., Shields, G. A., Tarbuck, G. M., He, T., Clarkson, M. O., and Wood, R. (2016): Effective use of cerium anomalies as a redox proxy in carbonate-dominated marine settings. Chemical Geology 438, 146-162.

Tsikos, H., Moore, J. M. and Harris, C. (2001): Geochemistry of the Paleoproterozoic Mooidraai Formation: Fe-rich limestone as end member of iron formation deposition, Kalahari Manganese Field, Transvaal Supergroup, South Africa. Journal of African Earth Sciences 32, no. 1, 19-27.

Van Kranendonk, M. J., Webb, G. E. and Kamber, B. S. (2003): Geological and trace element evidence for a marine sedimentary environment of deposition and biogenicity of 3.45 Ga stromatolitic carbonates in the Pilbara Craton, and support for a reducing Archaean ocean. Geobiology 1, 91-108.

Veizer, J. (1983): Chemical diagenesis of carbonates: theory and application of trace element technique, *in*: Arthur, M. A., Anderson, T. F., Kaplan, I. R., Veizer, J., Land, L. S. (Eds.): Stable Isotopes in Sedimentary Geology. Society of Economic Palaeontologists and Mineralogists Short Course 10, Tulsa.

Viehmann, S., Hoffmann, J. E., Münker, C. and Bau, M. (2013): Decoupled Hf-Nd isotopes in Neoarchean seawater reveal weathering of emerged continents. Geology 42, 2, 115-118; doi: 10.1130/G35014.1

Viehmann, S., Bau, M., Smith, A. J. B., Beukes, N. J., Dantas, E. L. and Bühn, B. (2015a): The reliability of ~2.9 Ga old Witwatersrand banded iron formations (South Africa) as archives for Mesoarchean seawater: Evidence from REE and Nd isotope systematics. Journal of African Earth Sciences 111, 322-334.

Viehmann, S., Bau, M., Hoffmann, J.E. and Münker, C. (2015b): Geochmistry of thw Krivoy Rog Banded Iron Formation, Ukraine, and the impact of peak episodes of increased global magmatic activity on the trace element composition of Precambrian seawater. Precambrian Research 270, 165-180.

Viehmann, S., Bau, M., Bühn, B. Dantas, E. L., Andrade, F. R. D. and Walde, D. H. G. (2016): Geochemical characterization of Neoproterozoic marine habitats: Evidence from trace elements and Nd isotopes in the Urucum iron and manganese formations, Brazil. Precambrian Research 282, 74-96.

Viers, J. and Wasserburg, G. J. (2004): Behavior of Sm and Nd in a lateritic soil profile. Geochimica et Cosmochimica Acta 68, 2043-2054.

von Blanckenburg, F., Mamberti, M., Schoenberg, R. Kamber, B. S. and Webb, G. (2008): The iron isotope composition of microbial carbonate. Chemical Geology 249, 113-128.

Webb, G. E. and Kamber, B. S. (2000): Rare earth elements in Holocene reefal microbialites: A new shallow seawater proxy. Geochimica et Cosmochimica Acta 64, 1557-1565.

Webb, G. E., Nothdurft, L. D., Kamber, B. S., Kloprogge, J. T. and Zhao, J. X. (2009): Rare earth element geochemistry of sceletarian coral skeleton during meteoric diagenesis: A sequence through neomorphism of aragonite to calcite. Sedimentology 56, 1433-1463.

Weyer, S., Münker, C. and Rehkämper, M. (2002): Determination of ultra-low Nb, Ta, Zr and Hf concentrations and the chondritic Zr/Hf and Nb/Ta ratios by isotope dilution analyses with multiple collector ICP-MS. Chemical Geology 187, 295-313.

Zakharov, D. O., Bindemann, I. N., Slabunov, A. I., Ovtcharova, M, Coble, M. A., Serebryakov, N. S. and Schaltegger, U. (2017): Dating the Paleoproterozoic snowball Earth glaciations using contomeporaneous subglacial hydrothermal systems. Geology; doi: 10.1130/G38759.1

Zhang, J. and Nozaki, Y. (1996): Rare Earth elements and yttrium in seawater: ICP-MS determinations in the East Caroline, Coral Sea, and South Fiji basins of the western South Pacific Ocean. Geochimica et Cosmochimica Acta 60, 4631-4644.

Zhang, J. and Nozaki, Y. (1998): Behaviour of rare earth elements in seawater at the ocean margin: a study along the slopes of the Sagami and Nankai troughs near Japan. Geochimica et Cosmochimica Acta 62, 1307-1317.

Zhong, S. and Mucci, A. (1995): Partitioning of rare earth elements (REEs) between calcite and seawater solutions at 25°C and 1 atm, and high dissolved REE concentrations. Geochimica et Cosmochimica Acta 59, 443-453.

FIGURES AND FIGURE CAPTIONS

Fig. 1: Locations of the sampling sites in the Transvaal Supergroup, Griqualand West Area, South Africa. The samples of Klipput dolostones originate from the farm *Sandridge*, those of Rooinekke limestones from the farm *Taaiboschfontein* (map modified after Frauenstein et al., 2009, and references therein).

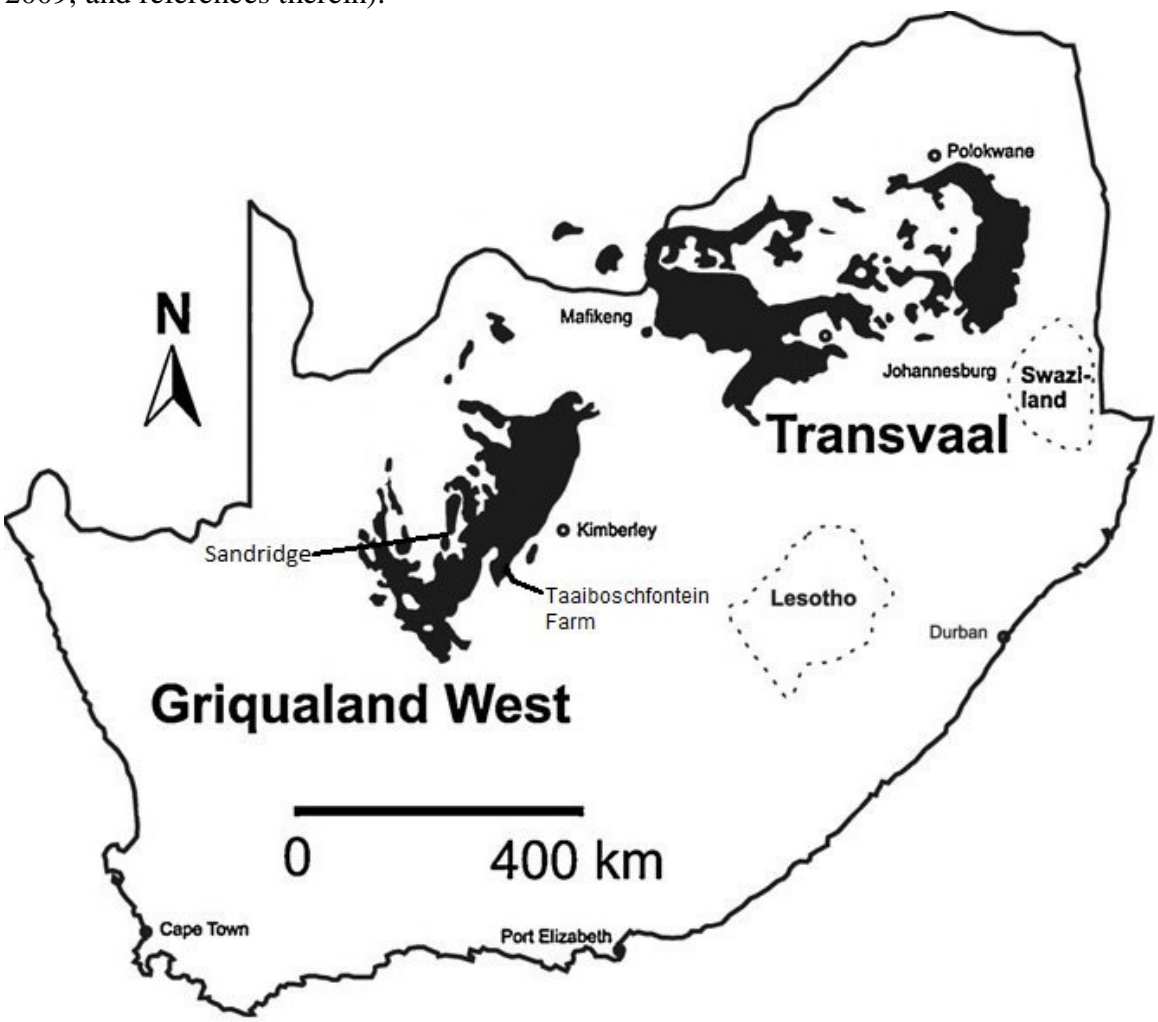

Fig. 2: General and detailed stratigraphy, respectively, of the (**a**) Transvaal Supergroup and (**b**) Koegas Subgroup in the Griqualand West Area, South Africa. Sampling locations are indicated by the blue stars in (**b**). Age information in (**a**) from [(a)] Bau et al. (1999), [(b)] Gutzmer and Beukes (1998), [(c)] Gumsley et al. (2017), [(d)] Nelson et al. (1999), [(e)] Pickard (2003), [(f)] Sumner and Bowring (1996).

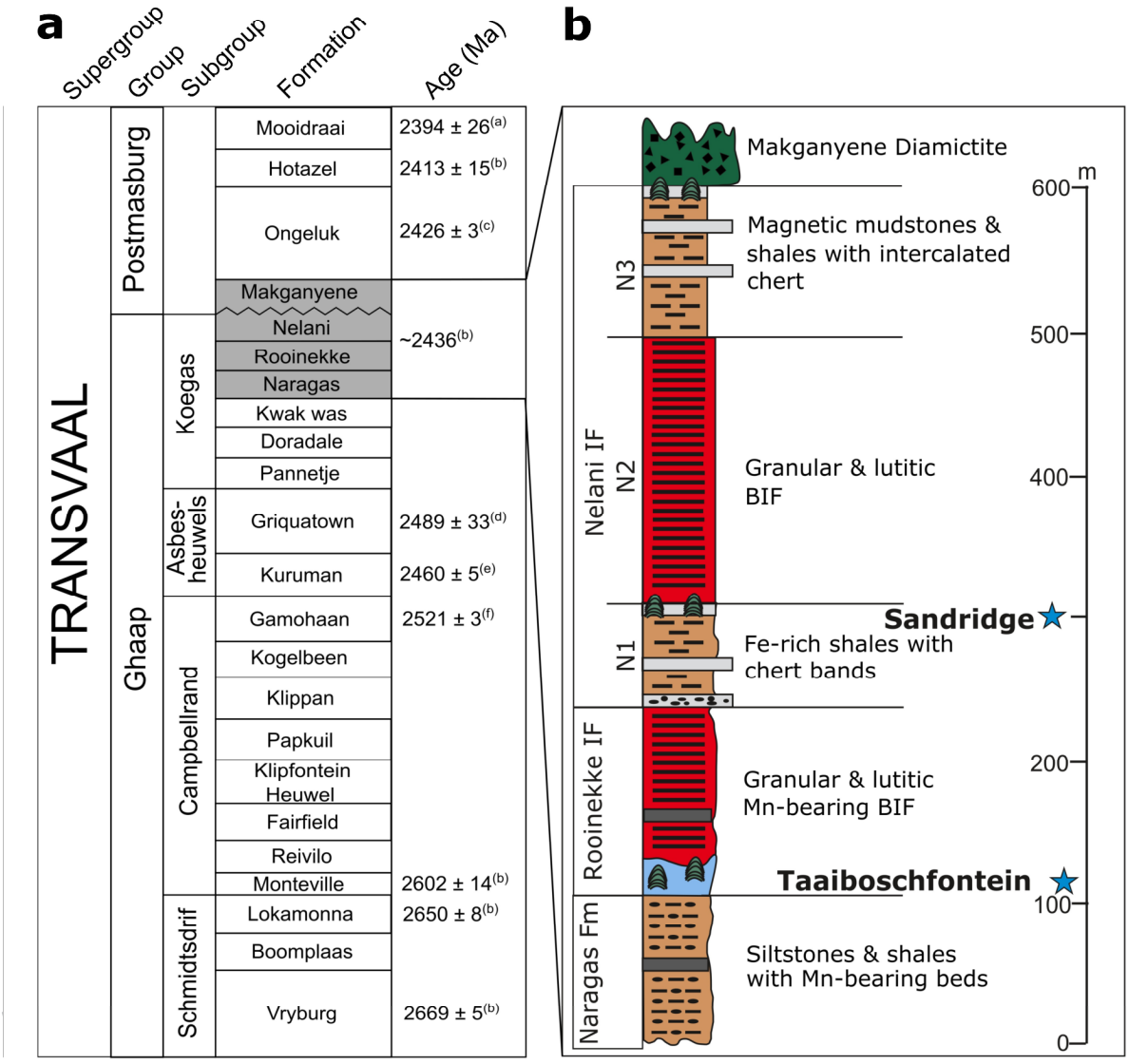

Fig. 3: Major element composition of stromatolitic limestones and dolostones from the Rooinekke and Nelani Formations, respectively, Transvaal Supergroup (South Africa), showing the clear distinction between the two different types of sedimentary carbonates.

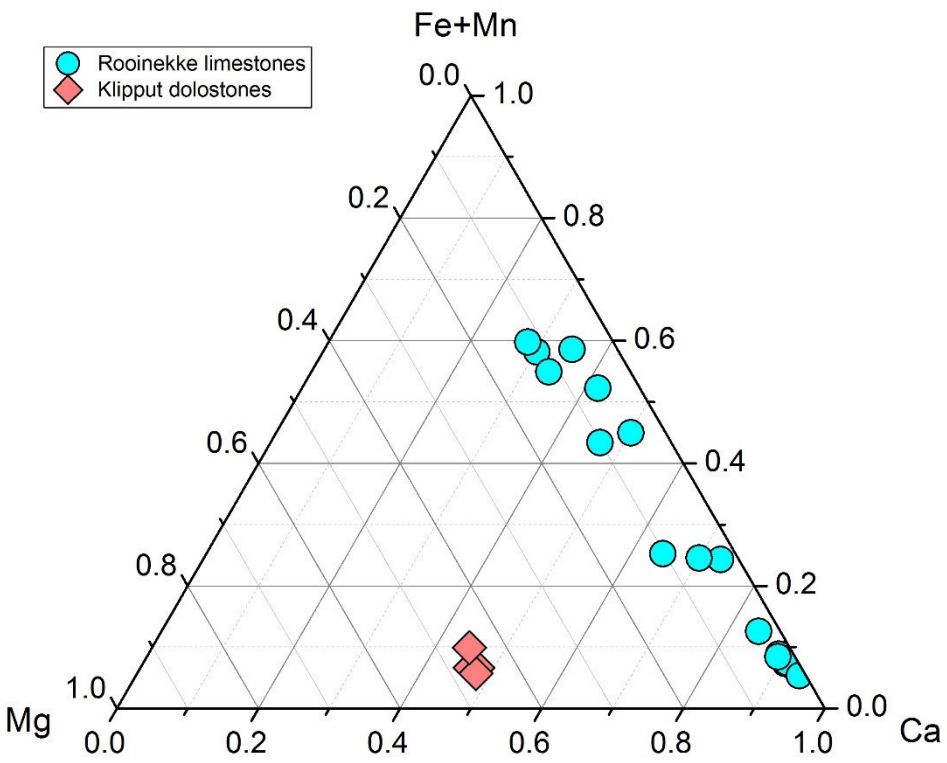

Fig. 4: REY_{SN} patterns of (**a**) Rooinekke limestones, (**b**) Klipput dolostones, (**c**) Campbellrand carbonates, and (**d**) Campbellrand microbialites and Kuruman and Penge iron formations (IF). The REY_{SN} patterns of Transvaal shales and modern shallow seawater are shown for comparison. Note the different scale in (**d**). Rooinekke limestones (**a**) show typical seawater characteristics such as positive La_{SN} and Gd_{SN} anomalies, super-chondritic Y/Ho ratios and an enrichment of the $HREY_{SN}$ relative to the $LREY_{SN}$. Klipput dolostones (**b**) show rather flat REY_{SN} patterns without distinctive seawater characteristics. In contrast to Rooinekke limestones, the older marine chemical sediments (**c** and **d**) show positive Eu_{SN} anomalies indicative of high-temperature hydrothermal input into ambient seawater. Open symbols in (**a**) and (**b**) denote samples exceeding the Al and Zr cutoff concentrations of 2000 ppm and 5 ppm, respectively.

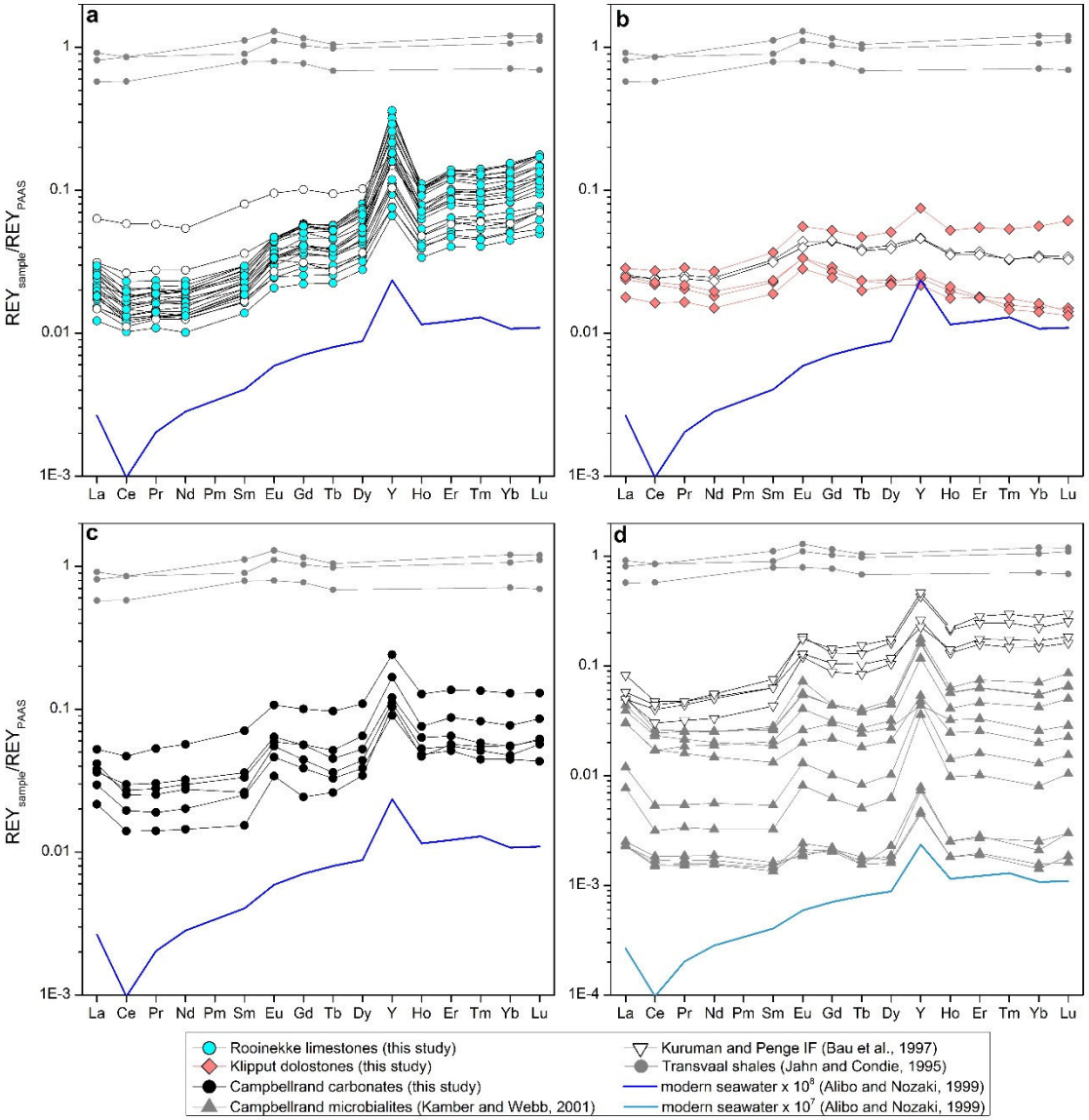

Fig. 5: Graph of (**a**) Al vs. Zr and (**b**) Al vs. Nd for Rooinekke limestones and Klipput dolostones from the Transvaal Supergroup, South Africa. (**a**) Al and Zr cutoff concentrations of 2000 ppm and 5 ppm (for further explanation see text) are indicated by the vertical and horizontal line, respectively. Open symbols denote samples that exceed these cutoff concentrations. Transvaal shales are shown for comparison (data from Jahn and Condie, 1995). (**b**) Two calculated mixing lines between an assumed endmember of the contemporaneous upper continental crust (represented by Transvaal shales from Jahn and Condie, 1995) with Al = 90,000 ppm and Nd = 25 ppm and two pure Rooinekke limestone endmembers, respectively. The tick marks represent admixture of 1 wt % and 10 wt % detrital material, respectively.

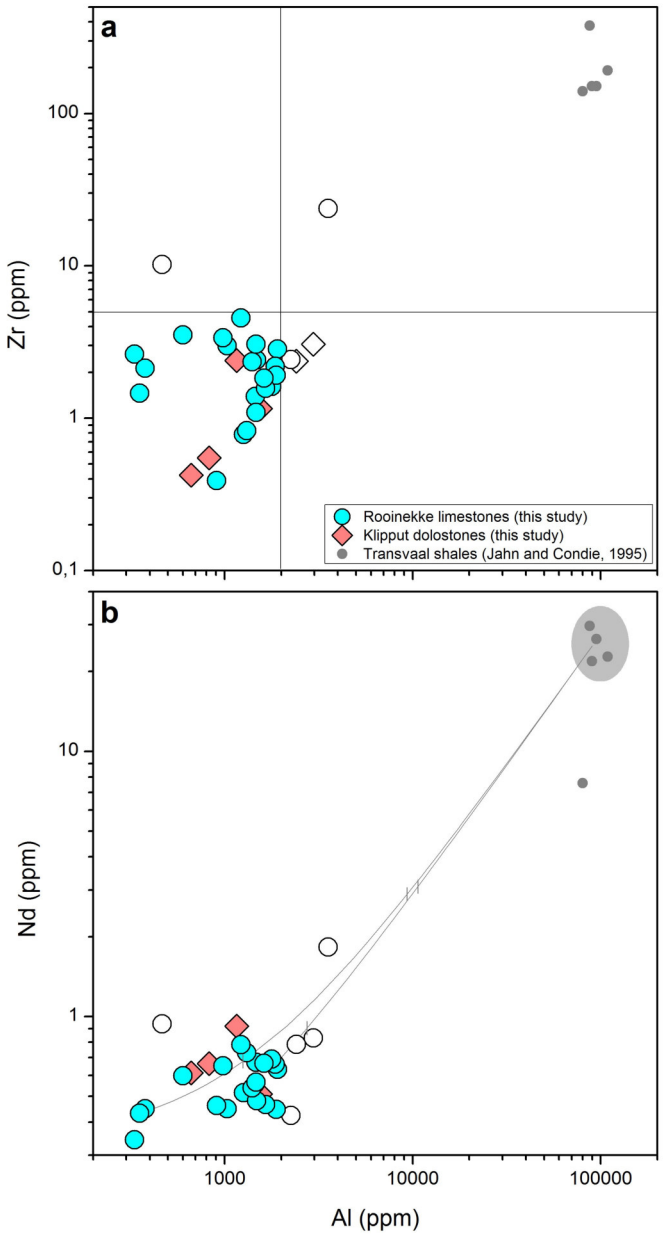

Fig. 6: Graph of (**a**) Y/Ho vs. $\varepsilon Nd_{(t)}$ and (**b**) $(Eu/Eu^*)_{SN}$ vs. $\varepsilon Nd_{(t)}$. (**a**) $\varepsilon Nd_{(t)}$ for Rooinekke limestones (t = 2440 Ma) and older marine chemical sediments (Campbellrand microbialites (t = 2521 Ma); Kamber and Webb, 2001, and Kuruman (t = 2460 Ma) and Penge (t = 2480 Ma) iron formation (IF); Bau et al., 1997). Transvaal shales ($\varepsilon Nd_{(2.44\ Ga)}$ recalculated from data of Jahn and Condie, 1995 and Dia et al., 1990; Y/Ho assumed to be similar to average upper continental crust of Rudnick and Gao, 2003) are shown for comparison. The lack of correlation between Y/Ho ratios and $\varepsilon Nd_{(t)}$ values for Rooinekke limestones indicates that their Nd isotope composition was not controlled by detrital aluminosilicates but was inherited from ambient seawater. Mostly negative $\varepsilon Nd_{(t)}$ values indicate a predominantly continental source for input of dissolved REY into Rooinekke seawater. (**b**) $(Eu/Eu^*)_{SN}$ vs. $\varepsilon Nd_{(t)}$ for Rooinekke limestones and older marine chemical sediments (Campbellrand microbialites from Kamber and Webb, 2001, and Penge and Kuruman IF from Bau et al., 1997). Campbellrand carbonates (this study) and younger Mooidraai carbonates (data from Tsikos et al., 2001, and Bau et al., 1999) are depicted as horizontal bars to illustrate values of $(Eu/Eu^*)_{SN}$ only; note that Nd isotope data for these samples are not available. Negative $\varepsilon Nd_{(t)}$ values for Rooinekke limestones and the absence of positive Eu_{SN} anomalies indicate continental REY sources to Rooinekke seawater instead of high-temperature hydrothermal sources. The latter are clearly present in the older Campbellrand carbonates (this study and microbialites from Kamber and Webb, 2001) and Kuruman and Penge IF but absent from younger Mooidraai carbonates. Shale data recalculated from Dia et al., 1990; $(Eu/Eu^*)_{SN}$ are not available and arbitrarily set to 1.

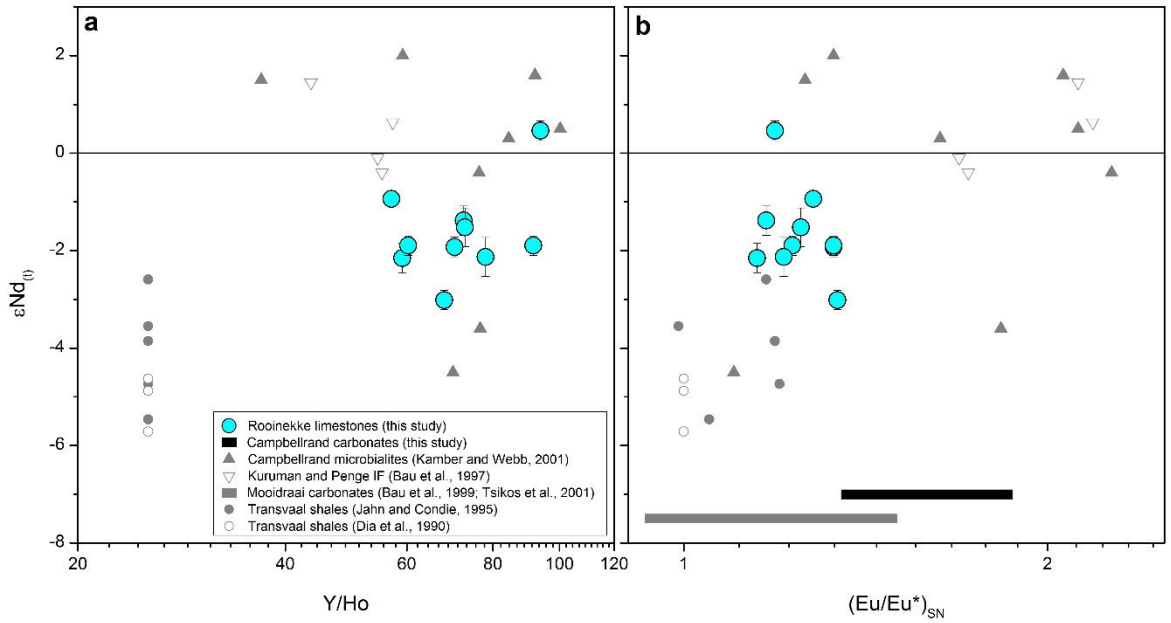

Fig. 7: Graph of (**a**) oxygen vs. carbon isotope compositions and (**b**) Fe/Ca ratios vs. carbon isotope composition of Rooinekke limestones and Klipput dolostones, Transvaal Supergroup (South Africa). Results for oxygen and carbon isotopes from this study agree well with those of Frauenstein et al., 2009.

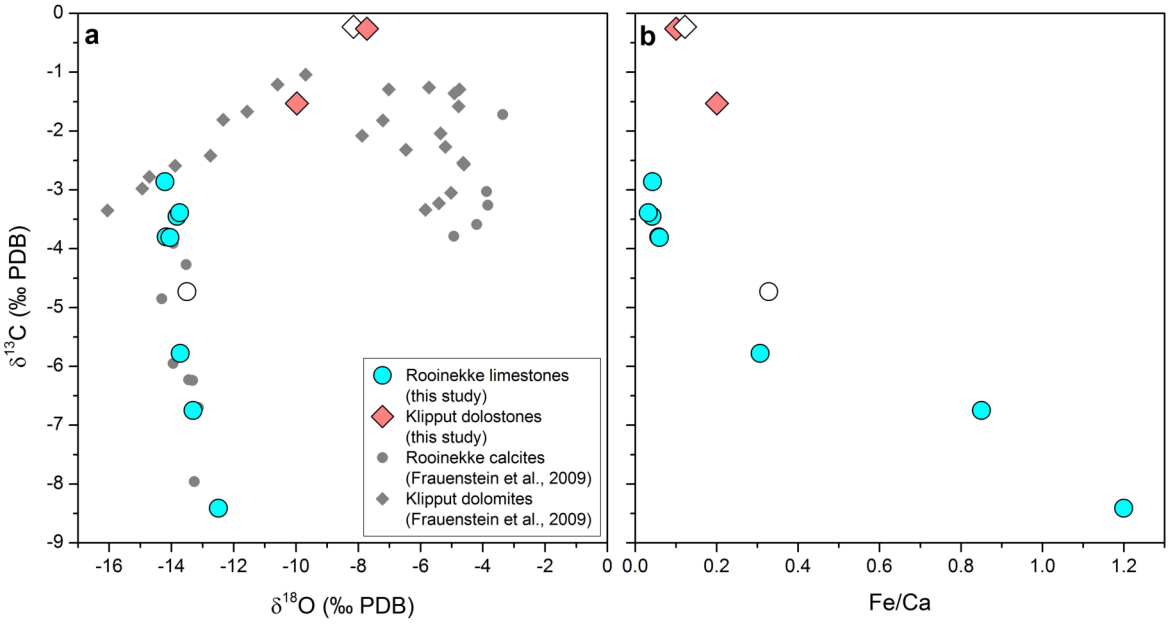

HIGHLIGHTS

- study of trace elements in 2.44 Ga old pure and pristine stromatolitic limestones
- reconstruction of paleo-chemistry of shallow seawater shortly before the GOE
- lack of negative Ce anomalies confirms anoxic conditions in shallow seawater
- lack of positive Eu anomalies shows fading input of high-temperature fluids
- Nd isotope composition of pure samples indicates continental REY sources